

# Atomic layer control in Sr-Cu-O artificial lattice growth

著者	花田 貴
journal or publication title	Applied Physics Letters
volume	65
number	13
page range	1717-1719
year	1994
URL	<a href="http://hdl.handle.net/10097/46974">http://hdl.handle.net/10097/46974</a>

doi: 10.1063/1.112896

# Atomic layer control in Sr-Cu-O artificial lattice growth

Ziyuan Liu<sup>a)</sup>

The Institute of Physical and Chemical Research (RIKEN), 2-1 Hirosawa, Wako-shi, Saitama 351-01, Japan, and Research Laboratory of Engineering Materials, Tokyo Institute of Technology, 4259 Nagatsuta, Midori-ku, Yokohama 227, Japan

Takashi Hanada, Rika Sekine, and Maki Kawai

The Institute of Physical and Chemical Research (RIKEN), 2-1 Hirosawa, Wako-Shi, Saitama 351-01, Japan

Hideomi Koinuma

Research Laboratory of Engineering Materials, Tokyo Institute of Technology, 4259 Nagatsuta, Midori-ku, Yokohama 227, Japan

(Received 17 May 1994; accepted for publication 21 July 1994)

Atomic layer growth control of the infinite-layer compound, SrCuO<sub>2</sub>, based artificial lattices is demonstrated on SrTiO<sub>3</sub> (100). Two different patterns have been observed by reflection high-energy electron diffraction during the alternating supply of strontium and copper metal under the flow of NO<sub>2</sub>. The intensity of the incommensurate streak increases with an increasing supply of Cu and decreases to zero with an increasing supply of Sr. Precise control of atomic layer growth is successfully carried out by *in situ* intensity monitoring of the incommensurate streak.

Among perovskite-type cuprate superconductors, the infinite-layer compound ACuO<sub>2</sub> (A=Ca,Sr,Ba), consists of CuO<sub>2</sub><sup>2-</sup> and A<sup>2+</sup> layers, is known as a parent structure. This system can be an electron carrier<sup>1-3</sup> superconductor or a hole carrier<sup>4-6</sup> superconductor depending on the dopant. Although the electron carrier system is realized in an ideal infinite-layer structure,<sup>7</sup> the hole carrier system, which is known to be a much higher temperature superconductor, is often accompanied by some superstructures along its *c* axis. The existence of Sr deficient layer in the superconductive infinite-layer compound was pointed out by Hiroi *et al.*<sup>6</sup> although the quantitative relationship with the volume fraction of the superconductors was not so clear.

Adachi *et al.*<sup>8</sup> has reported structures of 1.36 and 1.03 nm periods along the *c* axis in the superconductive phase, which is different from that of the infinite layer. Later, these periods were proved to be related to the existence of double alkaline earth layer in the infinite-layer structure.<sup>9</sup> Recently, Hiroi *et al.*<sup>10</sup> have reported a new family of cuprate superconductors described as Sr<sub>1+n</sub>Cu<sub>n</sub>O<sub>2n+1</sub>, having double SrO<sub>x</sub> layers along the *c* axis. There seem to be a general agreement that structural modification along *c* axis in the infinite-layer could be the cause of the superconductivity.

The atomic layer growth method is one of the most promising ways to construct a modulated structure along the *c* axis of the cuprate,<sup>11</sup> where a precise control of the layered growth is inevitable. This letter describes how an atomic layer controlled growth of infinite-layer structure is realized and demonstrates the introduction of double Sr layer into the infinite-layer structure.

A molecular beam epitaxial (MBE) growth was carried out in a chamber with base pressure of  $1 \times 10^{-10}$  Torr. NO<sub>2</sub> ( $5 \times 10^{-6}$ – $1 \times 10^{-5}$  Torr) was used as an oxidant. Strontium and copper were supplied from Knudsen cells, where the typical cell temperatures were 980 °C for Cu, and 360 °C for

Sr, and the deposition was controlled by the shuttering.

The surface of the substrate, SrTiO<sub>3</sub>(100) (Earth Jewelry Co., Ltd.) was cleaned by the Bi deposition/desorption method reported previously.<sup>12</sup> The surface structures of the substrate and the film were monitored *in situ* by reflection high-energy electron diffraction (RHEED) at a beam energy of 15 keV. The diffraction patterns observed by RHEED were acquired by a CCD camera, directly transferred to the computer, and the intensities of the diffraction streaks were monitored in real time. The structure of film formed was examined by x-ray diffraction (XRD).

The phase prepared by alternating supplies of Sr and Cu, under the atmosphere of NO<sub>2</sub> of  $5 \times 10^{-6}$ – $1 \times 10^{-5}$  Torr, depends heavily on the substrate temperature and the composition of Sr and Cu. When the temperature was higher than 380 °C, an orthorhombic SrCuO<sub>2</sub> phase, which is more stable than the tetragonal SrCuO<sub>2</sub> phase (infinite-layer structure), was obtained. When the temperature is lower than 310 °C, an amorphous phase was obtained. Only in the temperature range of 310–380 °C the tetragonal SrCuO<sub>2</sub> phase (infinite layer) was formed. Under the optimum temperature conditions, if the Cu supply exceeded 20% of the optimum ratio, the formation of CuO was observed, if the supply of Sr exceeded that of Cu, a phase of Sr<sub>2</sub>CuO<sub>3</sub> mainly grew. The infinite-layer compound, tetragonal SrCuO<sub>2</sub>, can be formed only in the temperature range of 310–380 °C and the Sr/Cu composition of 0.8–1.1. For the heterogeneous epitaxy, structure control of the interface is inevitable. In the case of the growth on SrTiO<sub>3</sub>(100), we have found<sup>13</sup> that at least two layers of SrO<sub>x</sub> have to be deposited between the TiO<sub>2</sub> layer of the substrate and the CuO<sub>2</sub> layer of the film.

During the growth of the tetragonal SrCuO<sub>2</sub>, two different RHEED patterns corresponding to the Sr-O and the Cu-O surface were observed. The RHEED patterns observed from the [110] direction of the SrTiO<sub>3</sub>(100) substrate are presented in Figs. 1(a) and 1(b). After the Sr supply (Sr-O surface), the pattern gives a  $1 \times 1$  structure [Fig. 1(a)], while that after the Cu supply (Cu-O surface) gives a clear feature of incommen-

<sup>a)</sup>Present address: Superconductivity Research Laboratory, ISTEC, 10-13 Shinonome 1-chome, Koto-ku, Tokyo 135, Japan.

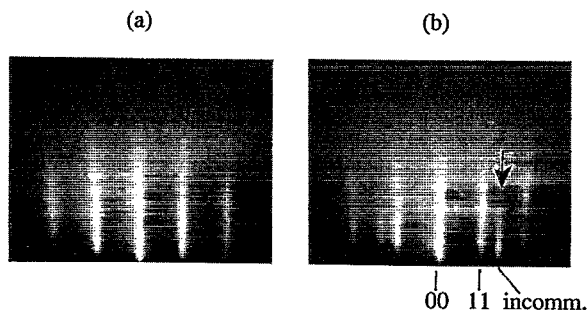


FIG. 1. RHEED patterns observed during the formation of the tetragonal  $\text{SrCuO}_2$  (infinite-layer structure). (a): The  $1 \times 1$  pattern observed after the Sr supply (Sr-O surface), and (b) the incommensurate pattern observed after the Cu supply (Cu-O surface).

surate streaks (shown by an arrow in the figure) in addition to the integer streaks [Fig. 1(b)]. The former streaks appear at the outside of every integer streaks with the distance from the integer streak being about  $\sqrt{2}-1$  times of that between neighboring integer. Every incommensurate streak appears to keep an identical distance from the integer streak. Similar incommensurate streaks with an identical feature were observed from the  $[100]$  direction as well. When the substrate showing the incommensurate streaks was cooled down to room temperature under the flow of  $\text{NO}_2$  ( $5 \times 10^{-6}$ – $1 \times 10^{-5}$  Torr), the pattern still remained, even increasing in intensity. This surface was examined by x-ray photoelectron spectroscopy (XPS). The  $\text{Cu}2p$  spectrum showed a clear feature of satellite structure telling us that the Cu was in the divalent state. Although the detailed structural origin of the incommensurate streaks observed for the Cu-O surface is not clear at the moment, the RHEED patterns for the Sr-O and that for the Cu-O surface clearly differs during the growth.

Figure 2 shows the intensity variation of the 11 streak and the incommensurate streak during the sequential growth. The intensity of the 11 streak increases as the Sr supply increases and decreases as the Cu supply increases as shown in Fig. 2(a). On the contrary, the intensity of the incommensurate streak decreases with the Sr supply and finally reaches to zero when the Sr layer is completed, then it increases to a certain degree with the Cu supply again [Fig. 2(b)]. Namely, the intensities of the 11 and the incommensurate streaks change in opposite manner. The intensity variation of the 11 streak is understood to be ascribed to the difference of the scattering factors of Sr and Cu atoms. Because the escape probability of electron exponentially decreases with the depth from the surface, the first layer dominates the intensity feature of the RHEED pattern. According to the table of Doyle and Turner,<sup>14</sup> the electron scattering factors for the  $\text{Sr}^{2+}$  ion is larger than the  $\text{Cu}^{2+}$  ion. With a large difference in the scattering factors, the intensity of the streaks reflects the dominant element on the surface.

Since the incommensurate streak is attributed to the superstructure of the Cu-O surface, the intensity depends mainly on the coverage of the Cu-O layer. Under a certain pressure of  $\text{NO}_2$ , the intensity of the incommensurate streaks depended only on the supplied amount of the Cu atoms on

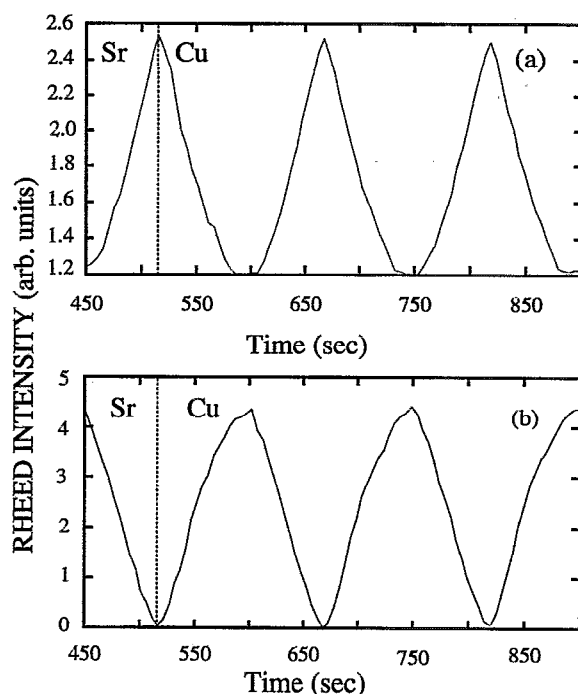


FIG. 2. The variation of the RHEED intensity with time during the formation of the tetragonal  $\text{SrCuO}_2$ . The intensity variation for (a) the 11 streak, and (b) the incommensurate streak.

the surface. Therefore, precise control of the elemental composition of Sr and Cu could be realized by monitoring the intensity of the incommensurate streaks. By supplying Sr until the intensity of the incommensurate streaks become zero, a precise deposition control of an atomic layer of Sr is realized. This is especially important when the deposition rate changes under the ambient  $\text{NO}_2$ . The supply of Cu can be controlled either by the deposition time or by monitoring the intensity of the incommensurate streak.

The XRD pattern of the  $\text{SrCuO}_2$  film with the thickness of 70 unit cells formed by the *in situ* composition control is shown in Fig. 3. The XRD pattern shows that the film is a single phase of tetragonal  $\text{SrCuO}_2$  with its  $c$  axis perpendicular to the surface of the substrate, where the  $c$  axis length was calculated from the 002 peak position to be 0.346 nm. The calculated XRD pattern of  $\text{SrCuO}_2$  film with the thickness of 70 unit cells is also shown in the bottom of the figure. It is clear that the observed pattern is in good agreement with the calculated value in its peak position and in the peak intensity ratio, indicating that the  $\text{SrCuO}_2$  film with nearly an ideal structure is formed.

Since the atomic layer growth of infinite-layer  $\text{SrCuO}_2$  phase is realized, efforts to introduce a structural modulation along the  $c$  axis have been carried out. After 10 unit cells of the infinite-layer  $\text{SrCuO}_2$  is formed, an extra Sr layer is introduced onto the Sr layer surface, and the sequence is repeated for seven times. The planned structure should correspond to the introduction of a double Sr layer for every 10 unit cells of  $\text{SrCuO}_2$ , namely  $[(\text{SrCuO}_2)_{10}\text{SrO}_x]_7$ . The XRD pattern of  $[(\text{SrCuO}_2)_{10}\text{SrO}_x]_7$  is shown in Fig. 4. Compared with the XRD pattern of the tetragonal  $\text{SrCuO}_2$  (Fig. 3), the

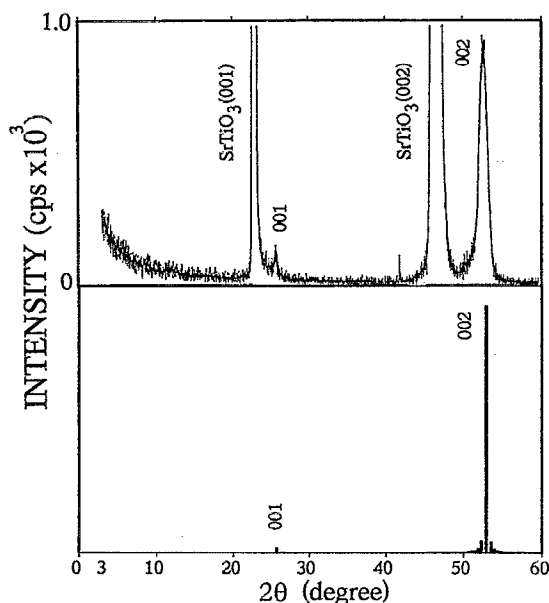


FIG. 3. The XRD pattern of the tetragonal  $\text{SrCuO}_2$  films with the thickness of 70 unit cells. Lower column is the calculated diffraction pattern with  $c=0.346$  nm and 70 unit cells.

pattern shown in Fig. 4 differs in the small angle region. Because the repetition of long unit cell  $[(\text{SrCuO}_2)_{10}\text{SrO}_x]$ , is limited to seven times, a clear feature of the diffraction function is observed. In addition, two small peaks are observed at  $2\theta=24.73^\circ$  and  $2\theta=26.69^\circ$  which are indexed to 0010 and 0011, respectively. The diffraction observed at  $2\theta=52.93^\circ$ , the most intense peak, which was indexed to 002 in the tetragonal  $\text{SrCuO}_2$ , is indexed to 0021. From the peak position, the lattice constant for the  $c$  axis is calculated to be 3.63

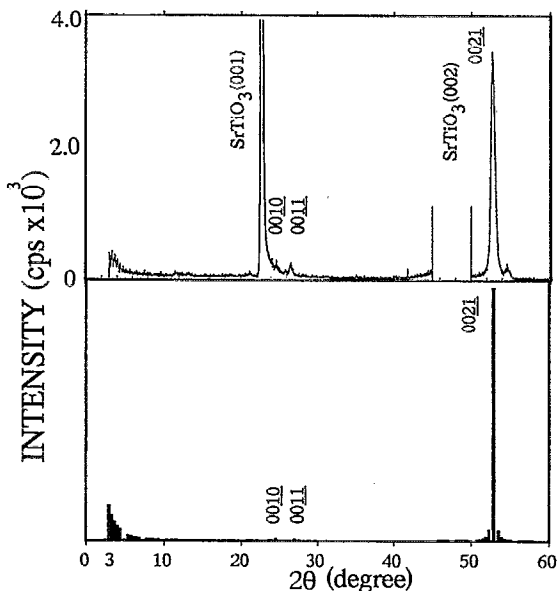


FIG. 4. The XRD pattern of the  $[(\text{SrCuO}_2)_{10}\text{SrO}_x]$  with seven units. Lower column is the calculated XRD pattern of  $[(\text{SrCuO}_2)_{10}\text{SrO}_x]$  with  $c=3.63$  nm.

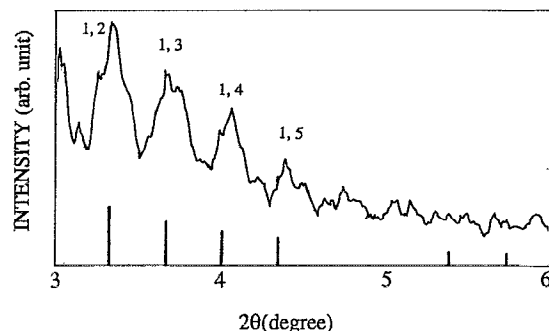


FIG. 5. The magnification of the small angle region of the XRD pattern in Fig. 4. Four peaks due to the diffraction function were clearly observed. The calculated peaks in the same angle region are shown by bar lines.

nm. The calculated XRD pattern of  $[(\text{SrCuO}_2)_{10}\text{SrO}_x]_7$  shown in the bottom of Fig. 4 is carried out using this value.

The small angle region of Fig. 4 is magnified in Fig. 5. The separation between these peaks are function of the product between the  $c$  axis value and the number of repetition. If we take the  $c$  axis value of 3.63 nm, which is obtained from the 0021 peak position, then the number of repetition calculated from the peak separation gives 6.9. The number obtained agrees with the sequence of the film, which is  $[(\text{SrCuO}_2)_{10}\text{SrO}_x]_7$ .

The transport properties of the films with the modulated structure have been published elsewhere.<sup>15</sup> The resistivity shows an anomaly at a temperature range of 100 and 80 K.

In summary, atomic layer controlled epitaxial growth of infinite-layer compound  $\text{SrCuO}_2$  is demonstrated. The  $\text{SrCuO}_2$  films with and without the modulated structure are formed by a precise control of the element supply utilizing the different feature observed in the RHEED patterns for different surfaces of Sr-O and Cu-O. The intensity monitoring of the incommensurate streaks observed for the Cu-O surface is shown to be a promising candidate for the atomic layer controlled growth of infinite-layer cuprates.

- <sup>1</sup> M. G. Smith, A. Manthiram, J. Zhou, J. B. Goodenough, and J. T. Markert, *Nature* **351**, 549 (1991).
- <sup>2</sup> G. Er, S. Kikkawa, F. Kanamaru, Y. Miyamoto, S. Tanaka, M. Sera, M. Sato, Z. Hiroi, M. Takano, and Y. Bando, *Physica C* **196**, 271 (1992).
- <sup>3</sup> G. Er, Y. Miyamoto, F. Kanamaru, and S. Kikkawa, *Physica C* **181**, 206 (1991).
- <sup>4</sup> M. Takano, M. Azuma, Z. Hiroi, and Y. Bando, *Physica C* **176**, 441 (1991).
- <sup>5</sup> M. Azuma, Z. Hiroi, M. Takano, Y. Bando, and Y. Takeda, *Nature* **356**, 775 (1992).
- <sup>6</sup> Z. Hiroi, M. Azuma, M. Takano, and Y. Takeda, *Physica C* **208**, 286 (1993).
- <sup>7</sup> J. D. Jorgensen, P. G. Radaelli, D. G. Hinks, and J. L. Wagner, *Phys. Rev. B* **47**, 14654 (1993).
- <sup>8</sup> S. Adachi, H. Yamauchi, S. Tanaka, and N. Mori, *Physica C* **208**, 226 (1993).
- <sup>9</sup> S. Adachi, H. Yamauchi, S. Tanaka, and N. Mori, *Physica C* **212**, 164 (1993).
- <sup>10</sup> Z. Hiroi, M. Takano, M. Azuma, and Y. Takeda, *Nature* **364**, 315 (1993).
- <sup>11</sup> X. Li, T. Kawai, and S. Kawai, *Jpn. J. Appl. Phys.* **31**, L934 (1992).
- <sup>12</sup> S. Watanabe, T. Hikita, and M. Kawai, *J. Vac. Sci. Technol. A* **9**, 2394 (1991).
- <sup>13</sup> Z. Liu, T. Hanada, M. Kawai, and H. Koinuma (unpublished).
- <sup>14</sup> P. A. Doyle and P. S. Turner, *Acta. Cryst.* **A 24**, 390 (1968).
- <sup>15</sup> M. Kawai, Z. Liu, R. Sekine, and H. Koinuma, *Jpn. J. Appl. Phys.* **32**, L1208 (1993).